WILEY

Magnetic resonance spectroscopy of fiber tracts in children with traumatic brain injury: A combined MRS – Diffusion MRI study

Emily L. Dennis[1,2] | Talin Babikian[2,10] | Jeffry Alger[3,4] | Faisal Rashid[1] |

Julio E. Villalon-Reina[1] | Yan Jin[1] | Alexander Olsen[2,5,6] | Richard Mink[7] |

Christopher Babbitt[8] | Jeffrey Johnson[9] | Christopher C. Giza[10,13] |

Paul M. Thompson[1,11] | Robert F. Asarnow[2,12,13]

[1]Keck School of Medicine, University of Southern California, Imaging Genetics Center, Mary and Mark Stevens Institute for Neuroimaging and Informatics, Marina del Rey, California

[2]Department of Psychiatry and Biobehavioral Sciences, Semel Institute for Neuroscience and Human Behavior, UCLA, Los Angeles, California

[3]Departments of Neurology and Radiology, UCLA, Los Angeles, California

[4]NeuroSpectroScopics LLC, Sherman Oaks, California

[5]Department of Psychology, Norwegian University of Science and Technology, Trondheim, Norway

[6]Department of Physical Medicine and Rehabilitation, St. Olavs Hospital, Trondheim University Hospital, Trondheim, Norway

[7]Department of Pediatrics, Harbor-UCLA Medical Center and Los Angeles BioMedical Research Institute, Torrance, California

[8]Miller Children's Hospital, Long Beach, California

[9]Department of Pediatrics, LAC+USC Medical Center, Los Angeles, California

[10]Dept of Neurosurgery and Division of Pediatric Neurology, Mattel Children's Hospital, UCLA Brain Injury Research Center, Los Angeles, California

[11]Departments of Neurology, Pediatrics, Psychiatry, Radiology, Engineering, and Ophthalmology, USC, Los Angeles, California

[12]Department of Psychology, UCLA, Los Angeles, California

[13]Brain Research Institute, UCLA, Los Angeles, California

Correspondence
Emily Dennis, Keck School of Medicine, University of Southern California, 2025 Zonal Ave, Los Angeles, CA, 90033
Email: emily.dennis@ini.usc.edu

Abstract

Traumatic brain injury can cause extensive damage to the white matter (WM) of the brain. These disruptions can be especially damaging in children, whose brains are still maturing. Diffusion magnetic resonance imaging (dMRI) is the most commonly used method to assess WM organization, but it has limited resolution to differentiate causes of WM disruption. Magnetic resonance spectroscopy (MRS) yields spectra showing the levels of neurometabolites that can indicate neuronal/axonal health, inflammation, membrane proliferation/turnover, and other cellular processes that are on-going post-injury. Previous analyses on this dataset revealed a significant division within the msTBI patient group, based on interhemispheric transfer time (IHTT); one subgroup of patients (TBI-normal) showed evidence of recovery over time, while the other showed continuing degeneration (TBI-slow). We combined dMRI with MRS to better understand WM disruptions in children with moderate-severe traumatic brain injury (msTBI). Tracts with poorer WM organization, as shown by lower FA and higher MD and RD, also showed lower N-acetylaspartate (NAA), a marker of neuronal and axonal health and myelination. We did not find lower NAA in tracts with normal WM organization. Choline, a marker of inflammation, membrane turnover, or gliosis, did not show such associations. We further show that multi-modal imaging can improve outcome prediction over a single modality, as well as over earlier cognitive function measures. Our results suggest that

demyelination plays an important role in WM disruption post-injury in a subgroup of msTBI children and indicate the utility of multi-modal imaging.

1 | INTRODUCTION

Diffusion magnetic resonance imaging (dMRI) can be used to reconstruct the white matter (WM) tracts of the brain and identify areas of brain damage after a traumatic brain injury (TBI). TBI can cause long-lasting disruptions to WM organization, which can be especially devastating in children and adolescents. While dMRI has good spatial resolution, it is limited in its ability to elucidate the processes underlying these disruptions. For example, reductions in fractional anisotropy (FA) often occur, which can reflect demyelination, inflammation, decreased axonal packing, or other changes to WM microstructure. DMRI studies of pediatric moderate to severe TBI (msTBI) completed more than a month post-injury generally show lower FA, higher mean diffusivity or apparent diffusion coefficient (MD or ADC), and higher radial diffusivity (RD; Dennis, Babikian, Giza, Thompson, & Asarnow, 2018).

Magnetic resonance spectroscopy (MRS) yields spectra that can reveal levels of neural metabolites such as N-acetylaspartate (NAA—a marker of neuronal and axonal integrity, which has a key role in oligodendrocyte and myelin production or repair [Cecil et al., 1998]) and choline (Cho—a marker of inflammation, membrane turnover, and gliosis; Ashwal et al., 2006). Previous single-voxel MRS studies of pediatric msTBI have shown decreases in NAA and increases in Cho at multiple time points post-injury, which correlate with cognitive outcome (Ashwal et al., 2000; Babikian et al., 2006; Babikian et al., 2010; Parry et al., 2004; Walz et al., 2008a; Yeo et al., 2006b). The majority of MRS studies employ a single voxel approach, but here we present results of a novel whole-brain MRS sequence (Ebel & Maudsley, 2003; Sabati et al., 2015). Our current whole-brain protocol allows us to integrate these data with other modalities, although it has poorer resolution for myo-inositol and glutamate/glutamine. By combining dMRI and MRS, disruptions in WM organization can be better related to biochemical alterations that might help identify their cause. In adults, studies including dMRI and MRS have shown some overlap between dMRI measures and MRS measures (Maudsley et al., 2015).

In our prior studies of pediatric msTBI, we identified two subgroups of msTBI patients based on a measure of the functional integrity of the corpus callosum—interhemispheric transfer time (IHTT) measured using visual event-related potentials (ERP; Ellis et al., 2015b). The msTBI group with slow IHTTs (TBI-slow) tended to have poor WM organization (Dennis et al., 2015a), which progressively worsened. The msTBI group (TBI-normal) with normal IHTTs showed minimal disruptions to WM organization, which improved longitudinally (Dennis, et al., 2017b). These groups did not significantly differ clinically or demographically so we sought to elucidate the processes underlying the WM disruption that some patients experience to better understand this divergence.

We collected dMRI and whole-brain MRS longitudinally post-injury. The dMRI and MRS data, collected in the same sessions, were co-registered for joint analyses. We used a method developed in our laboratory, autoMATE (automated multi-atlas tract extraction [Jin et al., 2014]) to extract FA, MD (mean diffusivity—the mean of all three eigenvectors), RD (radial diffusivity—the mean of the two non-primary eigenvectors), AxD (axial diffusivity—the primary eigenvector), NAA, and choline along tracts with common tract indices across subjects. We examined differences between each of the three groups (TBI-slow, TBI-normal, and healthy control) in these tract averages. We hypothesized that we would see lower NAA in those tracks where we found lower FA, specifically in the TBI-slow group. We hypothesized that elevations in choline would correspond to tracts with higher MD and RD.

2 | MATERIALS AND METHODS

2.1 | Participants

TBI participants were recruited from four Pediatric Intensive Care Units (PICUs) located in Level 1 and 2 Trauma Centers in Los Angeles County. In these institutions, patients with msTBI are routinely admitted to the PICU. A study representative discussed the goals of the study with the parents of patients, gave them an IRB-approved brochure about the study and obtained permission for the investigators to contact them after discharge from the PICU. Thirty-five percent of patients whose parents agreed to be contacted while the child was in the PICU participated in this study. Healthy controls, matched for age, sex, and educational level, were recruited from the community through flyers, magazines, and school postings.

Inclusion Criteria: (a) non-penetrating msTBI (intake or post-resuscitation GCS score between 3 and 12 or higher GCS with positive image findings); (b) 8–18 years of age at time of injury; (c) right-handed; (d) normal visual acuity or vision corrected with contact lenses/eyeglasses; and (e) English skills sufficient to understand instructions and be familiar with common words (the neuropsychological tests used in this study presume competence in English).

Exclusion Criteria: (a) history of neurological illness, such as prior msTBI, brain tumor or severe seizures; (b) motor deficits that prevent the subject from being examined in an MRI scanner (e.g., spasms); (c) history of psychosis, ADHD, Tourette's Disorder, learning disability, intellectual disability, autism, or substance abuse. These conditions were identified by parental report and are associated with cognitive impairments that might overlap with those caused by msTBI.

TABLE 1 Demographic information

| | TBI | | | | Healthy controls | |
| | TBI-slow | | TBI-normal | | | |
	Post-acute	Chronic	Post-acute	Chronic	Time 1	Time 2
N	15	9	14	9	23	21
F/M	5/10	2/7	3/11	2/7	12/11	7/14
IHTT avg. msec (SD)	25.6 (6.3)*	26.8 (6.3)*	7.9 (5.8)	8.5 (5.3)	9.4 (5.7)	9.7 (5.0)
Age avg. years (SD)	13.9 (2.3)	14.9 (2.0)	13.9 (3.2)	16.7 (2.8)	15.3 (2.8)	16.3 (3.2)
TSI weeks	12.0 (4.7)	61.2 (4.8)^	12.5 (5.1)	67.2 (6.1)	–	–
Interval	50.6 (5.9)		53.3 (10.0)		60.1 (11.9)	
GCS	9.6 (3.9)	7.7 (2.9)	8.3 (4.0)	9.4 (4.2)	–	–
EPTS	2	2	5	3	–	–
SAH	3	1	5	3	–	–
SDH	6	3	4	2	–	–
IVH	2	1	3	1	–	–
EDH	5	5	3	4	–	–
ICH	7	4	5	3	–	–
DAI	1	1	4	0	–	–
Contusion	5	3	1	3	–	–
ICP ↑	1	1	3	2	–	–
Dep Fx	4	3	5	2	–	–
ND Fx	5	3	3	3	–	–

We list the number of TBI (slow and normal IHTT TBI groups) and healthy control participants, the female/male ratio, the IHTT (inter-hemispheric transfer time, in ms), the average age (and standard deviation), time since injury (TSI; weeks), and interval between scans (in weeks) for participants who were included in both time points. In the TBI-normal group, 2 of the patients in the chronic phase did not contribute data in the post-acute phase. In the healthy controls, 6 of the participants in time 2 did not contribute data in the post-acute phase. We had acute CT information for 14/15 TBI-slow and 13/14 TBI-normal.

Abbreviations: GCS = Glasgow Coma Scale score upon hospital admission, EPTS = early post-traumatic seizures (seizure activity within 7 days post-injury, patients with post-traumatic epilepsy were excluded), SAH = subarachnoid hemorrhage, IVH = intraventricular hemorrhage, EDH = epidural hematoma, SDH = subdural hematoma, ICH = intracerebral hemorrhage, DAI = diffuse axonal injury, ICP ↑=increased intracranial pressure, Dep Fx = depressed skull fracture, ND Fx = non-depressed skull fracture.

* indicates a significant difference between the TBI-slow group and the healthy controls.

^ indicates a significant difference between the TBI-slow and TBI-normal groups. All 9 of the chronic TBI-slow participants contributed data in the post-acute phase, 7 of 9 chronic TBI-normal participants contributed data in the post-acute phase, and 15 of 21 time 2 healthy controls contributed data in the post-acute phase. Failure to contribute data to both time-points was due to poor quality MRS in some participants at time 1.

Participants were excluded if they had metal implants that prevented them from safely undergoing a MRI scan. Inclusion and exclusion criteria for the healthy controls were the same except for inclusion criterion #1.

We studied 29 children (21 male/8 female, average age = 13.9 years) with msTBI in the post-acute phase (2–5 months post injury) as well as 23 healthy control children (11 male/12 female, average age = 15.3 years). While the healthy control group was more balanced between males and females than the TBI group, this was not a significant difference. In the chronic phase (13–19 months post injury), we studied 18 children with msTBI and 21 healthy control children, most of whom had participated in the post-acute phase. Two msTBI patients and six healthy controls who participated in the chronic phase did not contribute data to the post-acute phase analyses, because of missing or poor-quality data. Demographic data are summarized in Table 1. The injury mechanisms for our TBI group were as follows: 7 motor-vehicle accident (MVA) – pedestrian, 6 MVA – passenger, 5 fall – skateboard, 2 fall – scooter, 2 fall – bike, 2 assault, 1 fall – skiing, 1 fall – ladder, 1 uncategorized blunt head trauma, and 1 unknown. The demographic information (see Table 1) from our sample is consistent with existing epidemiological information on moderate-severe pediatric/adolescent TBI, both in the male to female ratio and in the types of mechanisms of injury (Keenan & Bratton, 2006). From the CT scan that participants received at the hospital, the prevalence of CT findings was as follows across the 27/29 participants for whom we had clinical CT data: increased intracranial pressure (14%), diffuse axonal injury (18%), subarachnoid hemorrhage (28%), ventricular hemorrhage (18%), epidural hematoma (28%), subdural hematoma (39%),

intracerebral hematoma (50%), contusions (25%), skull fracture – any (68%), depressed skull fracture (36%), non-depressed skull fracture (32%).

2.2 | Scan acquisition

Participants were scanned on 3T Siemens Trio MRI scanners with whole brain anatomical and 72-gradient diffusion MRI (dMRI). Diffusion-weighted images were acquired with the following acquisition parameters: GRAPPA mode; acceleration factor PE = 2; TR/TE = 9500/87 ms; FOV = 256 × 256 mm; isotropic voxel size = 2 mm. Seventy-two images were collected per subject: 8 b_0 and 64 diffusion-weighted (b = 1,000 s/mm^2). 3D 1H magnetic resonance spectroscopic imaging was performed using an echo planar spectroscopic imaging (EPSI) pulse sequence. EPSI acquisition parameters were TR/TE 1710/70, spin echo slab excitation, slab thickness 135 mm, spatial sampling 50 × 50 × 18 over 280 × 280 × 180 mm^3, 1,000 spectral points with a spectral bandwidth of 1250 hz. The EPSI acquisition included interleaved water suppressed and water not suppressed volumetric acquisitions. EPSI data were processed using MIDAS software (Maudsley et al., 2006). Examples of image quality can be seen in (Babikian, et al., 2018).

2.3 | Scan comparison

Partway through the study, scanning moved from the UCLA Brain Mapping Center to the Staglin IMHRO Center for Cognitive Neuroscience, the same model and with the same scan parameters. Extensive testing was conducted with volunteer and phantom data to ensure no bias was introduced with respect to the study design. Details may be found in (Dennis, et al., 2015b).

2.4 | Cognitive assessment

Our cognitive performance index is a summary measure assessing multiple domains known to be affected in TBI (Babikian & Asarnow, 2009). It is a linear, unit weighted combination of the following age-based standardized measures: (a) Processing Speed Index from the WISC-IV/WAIS-III (Wechsler, 2003); (b) Working Memory Index from the WISC-IV/WAIS-III (Wechsler, 2003); (c) Trials 1–5 from the CVLT-C/II (Delis, Kramer, Kaplan, & Ober, 1994); and (d) Trial 4 from the D-KEFS (Delis, Kaplan, & Kramer, 2001). Further details of our performance index are found in (Moran et al., 2016).

2.5 | Tractography

AutoMATE (automated multi-atlas tract extraction), developed by our lab, is described fully in prior papers (Jin et al., 2014). Raw dMRI images were visually checked for artifacts, resulting in two participants being excluded from all analyses due to extensive slice dropout (not included in above participant count). DMRI images were corrected for eddy-current induced distortions using the FSL tool "eddy_correct" (http://fsl.fmrib.ox.ac.uk/fsl/). DMRI scans were skull-stripped using "BET" using default settings. FA and MD maps were computed using "dtifit".

Whole-brain dMRI tractography was performed with Camino (http://cmic.cs.ucl.ac.uk/camino/). The maximum fiber turning angle was set to 40°/voxel to limit biologically implausible results, and tracing stopped when fractional anisotropy (FA) dropped below 0.2, as is standard in the field.

2.6 | Fiber clustering and label fusion

As part of autoMATE, five WM tract atlases were constructed from adolescents in the study (2 female/3 male, 14–18 years old, all healthy controls), following procedures detailed previously for other atlases (Jin et al., 2014). These atlases, based on the "Eve" brain atlas (Zhang et al., 2010), include 19 major WM tracts: the bilateral corticospinal tract, bilateral cingulum, bilateral inferior fronto-occipital fasciculus, bilateral inferior longitudinal fasciculus, bilateral uncinate, bilateral parahippocampal cingulum, left arcuate fasciculus (the right arcuate is too asymmetric for population studies to be practical [Catani, et al., 2007]), and corpus callosal tracts divided into six segments—frontal, precentral gyrus, postcentral gyrus, parietal, temporal, and occipital. The Eve atlas was registered, linearly and then non-linearly, to each subject's FA map using ANTs (advanced normalization tools [Avants et al., 2011]) and its regions of interest (ROIs) were correspondingly warped to extract 19 tracts of interest for each subject based on a look-up table (Zhang et al., 2010). ROI registration was visually checked for all subjects, and all passed quality control. The purpose of the Eve atlas was registration of ROIs used for tract identification. The purpose of the five study-specific atlases was tract refinement and fusion.

Each subject's FA map was further registered non-linearly to each of the five manually constructed atlases. All registrations were visually inspected for quality, and all passed quality control. The 19 tracts from each atlas were then warped to the subject space based on the deformation field from the above-referenced registration steps (Jin et al., 2011). We refined fiber extractions of each tract based on the distance between the warped corresponding tract of each atlas and the subject's fiber candidates from ROI extraction. Individual results from the five atlases were fused. We visually inspected the resulting fiber bundles. For each of the 19 WM tracts, we selected one example subject to display results of group analyses. Fractional anisotropy (FA) is the degree to which water is diffusing preferentially in one direction (along axons). MD (mean diffusivity, also called apparent diffusion coefficient) is a related measure of the average diffusivity across all three primary eigenvectors and typically increases when FA decreases. We extracted tract-based FA, MD, RD, and AxD at this point.

2.7 | MRS registration

The MRS images were extracted with MIDAS software. These images display water-referenced metabolite (i.e., NAA and Cho) concentration using an institutional unit system that can be applied across subject. For each subject, the T1 image that was extracted with the MRS images was linearly aligned to the $b0$ image. These transformations were applied to the MRS images, to reduce resampling and data loss. The water image extracted along with the metabolite images was

aligned to the *b0* in the same way, and this transformation was applied to the spatial derivative of the B0 (grad B0—N.B. this is a separate measurement from the dMRI *b0*, the B0 is also the magnetic field strength), which provided B0-inhomogeneity for use as a spectral quality indicator (regions of high B0-inhomogeneity and therefore low spectral quality are excluded from analysis as described below—the frontal and mesial temporal areas are more prone to poor quality spectra). The threshold used for exclusion is 0.07 ppm/cm. The water image was used to register the thresholded B0 image as it is a better registration target. Once the MRS images were registered to the *b0*, they were masked by the grad B0 file, which was also registered to the *b0*. These registrations were visually quality controlled.

We now had NAA and Cho images, with areas of high spatial B0 inhomogeneity masked out, that were well-registered to the dMRI data and could be worked through the autoMATE pipeline, as was done for FA, MD, RD, and AxD. This gave us NAA and Cho along the same coordinates/indices. For all six measures (FA, MD, RD, AxD, NAA, and Cho) we also generated tract averages, averaging each measure across all indices along a given tract to yield 19 summaries for each measure. All analyses focused on tract averages to compensate for the difference in resolution between the dMRI and MRS scans.

2.8 | TBI subgroups

We previously found a subgroup within the msTBI patient population, based on a visual evoked potential (VEP) measure of interhemispheric transfer time (IHTT; Dennis et al., 2015a; Ellis et al., 2015a) that we used to measure the functional integrity of the corpus callosum. Roughly half of the msTBI patients had IHTTs within the healthy control range (shorter than 18 ms), while the other patients had significantly longer IHTTs. These significant differences in IHTT can be seen in Table 1. In the first few months post-injury, some msTBI patients have significantly impaired callosal functional and structural integrity, and this affects cognitive performance as well. Additionally, these differences appear to be progressive, as one subgroup experiences expanding WM disruption and atrophy while the other subgroup of msTBI children appears to begin to return to a healthy trajectory (Dennis, et al., 2017a; Dennis, et al., 2017b). Importantly, the subgroup with impaired callosal function does not differ from the other msTBI patients in demographic or acute injury variables (including the incidence of lesions as detected by acute CT). In all analyses on this dataset, we have examined the msTBI group as two groups—TBI-slow (those with significantly longer IHTTs) and TBI-normal (those with IHTTs in the normal range).

2.9 | Statistical analyses

2.9.1 | Group differences

AutoMATE yields matrices containing FA, MD, RD, AxD, NAA, or Cho at consistent indices across participants, which we average within each tract, and these are the input for our analyses. For investigating group differences, we run linear regression in the form:

$$\text{dMRI} \sim A + \beta_{Group}\text{Group} + \beta_{Age}\text{Age} + \beta_{Sex}\text{Sex} + \beta_{Scanner}\text{Scanner} + \varepsilon \tag{1}$$

where dMRI is FA, MD, RD, AxD, NAA, or Cho averaged across a given tract, A is the constant WM integrity term, the βs are the covariate regression coefficients, and ε is an error term. In this regression, we are including covariates for age, sex, and scanner. Group is a binary dummy variable—we ran analyses separately testing for differences between TBI-slow and controls, TBI-normal and controls, and between TBI-slow and TBI-normal. All statistical tests are corrected for multiple comparisons using FDR (Benjamini & Hochberg, 1995) across all tracts, all measures, and all three comparisons (TBI-slow vs. TBI-normal, TBI-slow vs. control, TBI-normal vs. control) tested.

2.9.2 | Partial F-test

We ran a partial *F*-test comparing a full model to reduced models to see the added contribution of MRS in predicting cognitive outcome. In a prior paper, we showed that a model including IHTT and dMRI was more predictive of later cognitive function than a model with either variable alone. Here we examined the impact of MRS in the model. The models we compared were:

$$\text{Model \#1 : Time 2 Cognitive function} \sim \text{MRS}$$

$$\text{Model \#2 : Time 2 Cog. func.} \sim \text{MRS} + \text{dMRI}$$

$$\text{Model \#3 : Time 2 Cog. func.} \sim \text{MRS} + \text{dMRI} + \text{IHTT}_{Group}$$

$$\text{Model \#4 : Time 2 Cog. func.} \sim \text{MRS} + \text{dMRI} + \text{IHTT}_{Group} + \text{Time 1 Cog. func.}$$

DMRI is FA, MD, RD, or AxD for a given tract, and MRS is NAA or Cho for the same tract. The outcome is a *F*-statistic, indicating in which tracts the additional variable increased the amount of explained variance in cognitive outcome. We compared Model #2 to Model #1, Model #3 to Model #2, and Model #4 to Model #3. These analyses were corrected for multiple comparisons across all tracts tested.

3 | RESULTS

There were minimal significant differences when comparing TBI-slow and TBI-normal to each other in FA, MD, RD, AxD, NAA, or Cho. The TBI-normal group had significantly higher NAA than the TBI-slow group in the post-acute phase in the right parahippocampal cingulum. In the chronic phase, the TBI-slow group had higher AxD in the parietal corpus callosum than the TBI-normal group. Each TBI group showed significant differences compared to the healthy controls. Significant differences between healthy controls and both groups at both time points are shown in Figure 1. The TBI-slow group showed disrupted WM organization (in lower FA and/or higher MD or RD) across many tracts, which we have shown in prior papers as well (Dennis et al., 2015a; Dennis, et al., 2017b). They also showed lower NAA compared to healthy controls, but only in tracts where we found disrupted WM organization: five tracts 2–5 months post-injury and four tracts 13–19 months post injury showed lower NAA in the TBI-slow group, all of which also showed lower FA, higher MD, and/or higher RD. We did not find lower NAA in the TBI-slow group compared to controls in
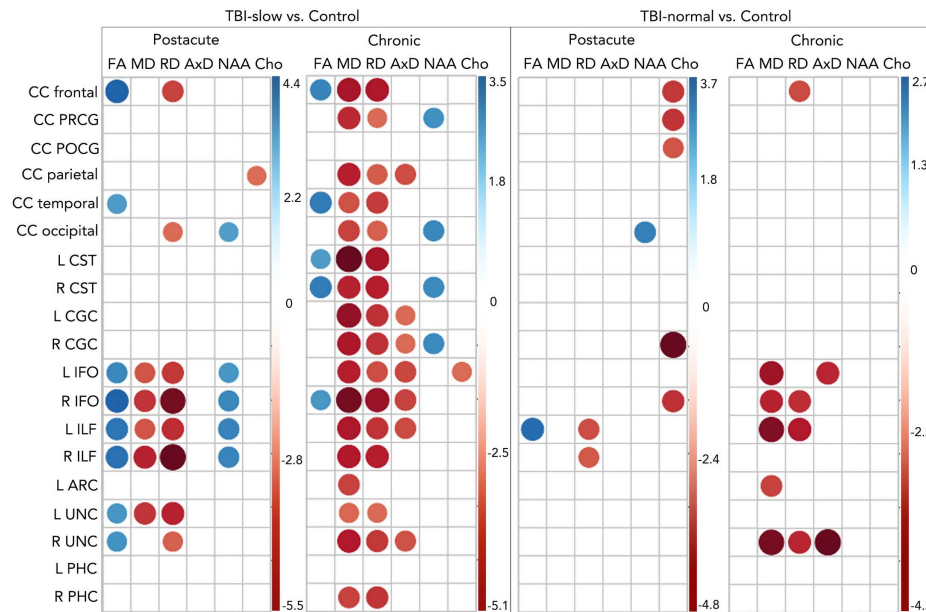
FIGURE 1 Post-acute and chronic differences between TBI-slow and control (left panels), and between TBI-normal and control (right panels). The color corresponds to the T statistic from each regression, as indicated in the color bars for each panel, with blue indicating higher values in controls and red higher values in TBI. The size of the circle corresponds to the magnitude of the T-stat. Only significant T-stats are included (after correction for multiple comparison across tracts, measures, and comparisons, FDR ($q < 0.05$) [Color figure can be viewed at wileyonlinelibrary.com]

WM tracts with normal WM organization. This suggests that dMRI and NAA are assessing similar processes. Five tracts showed higher choline in TBI-normal relative to healthy controls in the post-acute phase, but none of these showed disruptions in WM organization, which may reflect inflammation but could also indicate cellular turnover during recovery. We previously found increased levels of choline in global measures of cortex in both msTBI subgroups 2–5 months post-injury (Babikian et al., 2018).

We ran a partial F-test to examine the joint contributions of dMRI, MRS, and IHTT in predicting long term cognitive outcome. We compared four models: one including only MRS variables from time 1, the second adding dMRI variables from time 1, the third adding IHTT group (TBI-slow, TBI-normal, or control), and the final model including time 1 cognitive performance. The outcome variable was an index of cognitive performance (Moran et al., 2016) at the chronic time-point (13–19 months post-injury). NAA alone was a poor predictor of cognitive function (adjusted R-squared values shown in Table 2). Adding FA to the model significantly improved the amount of variance in long-term cognitive outcome for 13 of the 19 tracts. Adding IHTT group added further improvement to outcome prediction, for all 19 tracts. Finally, including time 1 cognitive function in combination with all three measures (MRS, dMRI, and IHTT) significantly improved outcome prediction across all 19 tracts. We additionally computed AIC (Akaike information criterion, Akaike, 1974) for each model within tract, also included in Table 2. With the addition of each variable, the AIC value decreased, indicating an improvement in model fit. Not surprisingly, time 1 cognitive function is the best individual predictor of chronic cognitive function, with an adjusted R^2 value of 0.757. However, the combination of MRS, dMRI, and IHTT explained a significant amount of variance in

chronic cognitive function. Comparing the full model (Model 4) to a model using time 1 cognitive function only still yielded significant F-statistics for all tracts with the exception of the left corticospinal tract, left inferior longitudinal fasciculus, and left parahippocampal cingulum. Figure 2 shows the adjusted R^2 values for the model including NAA, FA, and IHTT.

4 | DISCUSSION

In prior papers we have shown that a subgroup of pediatric msTBI patients experiences a progressive decrease in WM organization (Dennis, et al., 2017b). However, with only dMRI data, we were not able to determine whether these deficits were due to demyelination, inflammation, or other changes in neuronal organization. In this paper, we integrated complementary information from dMRI and MRS to better understand WM disruption post-injury and improve outcome prediction. Our results do not fully answer the question of the cause of pathology, but shed some light on this question and give us a starting point to build future analyses on. We focused on tracts where there were differences in WM organization between the msTBI patients who showed progressive decrease in WM organization (the TBI-slow group) compared to controls. Differences in NAA in those WM tracts corresponded to differences in dMRI measures, while choline did not show a similar correspondence with WM organization. We did not find lower NAA in the TBI-slow group compared to controls in WM tracts with normal WM organization. NAA is a trophic, neuronally-derived metabolite that is transferred to oligodendrocytes for use in myelination and myelin repair. NAA may act as a reservoir of acetate for coenzyme A synthesis which, when disrupted by msTBI, compromises energy

TABLE 2 AIC and Adjusted R^2 values for all models

	Model 1 AIC	Model 1 Adj. R^2	Model 2 AIC	Model 2 Adj. R^2	Model 3 AIC	Model 3 Adj. R^2	Model 4 AIC	Model 4 Adj. R^2
CC frontal	398.54	0.0244	395.31	**0.3423**	377.79	**0.3852**	330.99	**0.7937**
CC prcg	399.39	0.0073	397.16	**0.0806**	385.39	**0.2819**	332.27	**0.7583**
CC pocg	398.39	0.0274	396.35	0.0309	385.27	**0.2837**	333	**0.7574**
CC parietal	394.08	0.1093	393.88	**0.1705**	381.65	**0.3347**	332.51	**0.7587**
CC temporal	393.29	0.1235	392.91	**0.1888**	382.55	**0.3225**	331.03	**0.7655**
CC occipital	390.78	0.1674	390.42	**0.2508**	380.15	**0.3548**	330.37	**0.7683**
L CST	399.81	−0.0013	397.66	−0.0153	386.75	**0.2618**	334.05	**0.7536**
R CST	400.64	−0.0182	398.76	−0.0396	385.47	**0.2809**	331.53	**0.7651**
L CGC	399.08	0.0135	396.82	**0.1064**	383.14	**0.3141**	333.02	**0.7724**
R CGC	396.01	0.0736	394.11	**0.1064**	383.43	**0.3102**	332.28	**0.7677**
L IFO	400.55	−0.0164	398.48	0.0157	387.28	**0.2538**	329.77	**0.7650**
R IFO	400.07	−0.0066	398.07	**0.0379**	387.2	**0.2550**	332.79	**0.7623**
L ILF	400.41	−0.0135	398.39	**0.0514**	386.92	**0.2591**	332.52	**0.7538**
R ILF	400.15	−0.0082	398.5	0.0066	386.82	**0.2607**	332.95	**0.7554**
L ARC	400.72	−0.0201	398.87	**0.1169**	383.41	**0.3104**	332.1	**0.7656**
L UNC	399.99	−0.0049	398.87	**0.1769**	383.49	**0.3093**	330.18	**0.7706**
R UNC	400.3	−0.0114	399.03	**0.1026**	385.92	**0.2741**	334	**0.7703**
L PHC	399.47	0.0058	397.83	0.0183	386.97	**0.2585**	334.2	**0.7479**
R PHC	400.65	−0.0185	398.89	**0.0361**	386.64	**0.2634**	333.06	**0.7577**

Model #1 included only Time 1 NAA (averaged within each ROI). Model #2 included Time 1 NAA and Time 1 FA. Model #3 included Time 1 NAA, Time 1 FA, and IHTT group. Model #4 included Time 1 NAA, IHTT group, Time 1 FA, and Time 1 cognitive performance. The outcome variable in all cases was Time 2 cognitive performance. Bolded entries in the R^2 columns are those with significant F-statistics when compared to the prior model (Model 4 vs. Model 3, Model 3 vs. Model 2, Model 2 vs. Model 1).
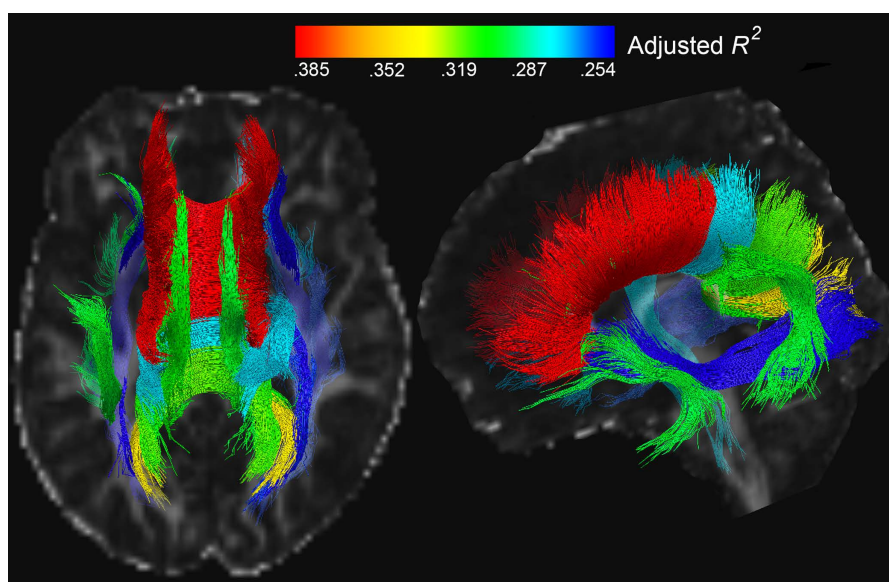

FIGURE 2 Adjusted R^2 values for the model including NAA, FA, and IHTT at Time 1, predicting cognitive function at Time 2. The color of the tract corresponds to the R^2 value, as shown in the color bar

derivation, lipid synthesis and protein acetylation (Moffett, Arun, Ariyannur, & Namboodiri, 2013). This in turn reduces myelin repair. The decreases in FA, along with increases in MD and RD suggest demyelination/absence of myelin repair, rather than axonal degeneration (Sidaros et al., 2008; Song et al., 2005). A number of studies have shown alterations in MD and RD predominately in the chronic phase, rather than FA (Dennis et al., 2015b; Wilde et al., 2012). Higher MD and RD, in the absence of significant differences in FA, suggest that there may also be higher AxD, albeit not significantly higher. This may indicate that some level of microstructural re-organization is occurring.

There was a lack of correspondence between choline and dMRI measures in WM tracts in our results. Most prior MRS studies in pediatric msTBI were completed in the first month post-injury (Ashwal et al., 2004; Ashwal et al., 2000; Babikian et al., 2006; Brenner, Freier, Holshouser, Burley, & Ashwal, 2003; Holshouser et al., 1997; Holshouser, Tong, & Ashwal, 2005; Yeo et al., 2006a), and many examined NAA and Cho normalized by Cr (creatine). However, evidence suggests that Cr is not as stable post-injury as initially thought (Li, Wang, & Gonen, 2003), which is why we examined unnormalized NAA and Cho. Only a few papers have examined MRS measures after the first month post-injury (Babikian et al., 2010; Parry et al., 2004; Walz, et al., 2008b). Both of these differences could impact comparability between our data and prior studies. Within the GM, two studies have found lower NAA in TBI (Ashwal et al., 2000; Holshouser et al., 1997), and one found lower NAA/Cho and higher Cho/Cr in patients with a bad outcome as compared to those with a good outcome (small sample: 11 subjects total; Brenner et al., 2003). In the WM, studies have similarly shown lower NAA and higher Cho in TBI (Babikian et al., 2010; Parry et al., 2004). We found higher Cho in some areas, but these differences did not overlap with dMRI differences, and were less extensive compared to NAA differences. Studies examining both GM and WM generally show lower NAA in WM (Ashwal et al., 2006; Holshouser et al., 2005) and higher Cho in both GM and WM (Ashwal et al., 2006). Acute NAA in both GM and WM are predictive of outcome (Babikian et al., 2006), but chronically Cho in GM shows more associations with neurobehavioral function than NAA levels or metabolite levels in WM (Walz et al., 2008b). In a recent analysis, we found elevated choline in both msTBI groups at the post-acute phase, but it remains high at 16 months post-injury in the TBI-normal group (Babikian et al., 2018). While this could indicate continuing inflammation, it could also indicate cellular turnover and recovery processes. It is possible that the choline signal reflects different processes at different stages post-injury, perhaps differentially across tissue types as well. While we cannot answer this with our current data, in the future we will collect a new MRS sequence that will allow us to measure additional metabolites—myo-inositol and glutamate/glutamine. Myo-inositol can reflect blood-brain barrier compromise and inflammatory processes, while the glutamate/glutamine ratio is altered due to the energy crisis that occurs immediately post-injury, as is correlated with outcome (Shutter, Tong, & Holshouser, 2004). There have not been many investigations combining dMRI and MRS, especially in a pediatric population. One recent paper in a healthy cohort showed maturational changes in dMRI and MRS measures, but did not find strong correlations between dMRI and MRS values (Ghosh et al., 2017).

In our previous paper, we showed that IHTT and dMRI information together explain more variance in cognitive function than either alone (Dennis et al., 2015a); here we extended this to include MRS. A model including functional (IHTT), structural (dMRI), metabolic (MRS), and prior cognitive information can predict long-term cognitive outcome better than any reduced model, indicating that the imaging modalities provide complementary information. One thing to note is that the IHTT variable partially reflects the TBI group difference. MRS and dMRI information from the corpus callosum (frontal, parietal, occipital and temporal), cingulum, uncinate, and arcuate appeared to be most useful in explaining variance in long-term cognitive function (**Figure** 2, adjusted R^2 values > .30). Multi-modal imaging information from the frontal corpus callosum was the most predictive, which makes sense as it facilitates communication among many higher-level cognitive processing regions. Time 1 cognitive function was individually the most predictive variable of time 2 cognitive function unsurprisingly, but the addition of multi-modal imaging information still yielded a significant improvement in prediction accuracy for most of the tracts. **Figure** 2 is only showing the imaging variables to convey the joint power of multi-modal imaging information. Cognition is supported by a complex network of neural systems. With more accurate outcome models, we may detect factors that aid recovery and possible points of intervention. Accurate outcome models also aid clinicians in identifying patients at higher risk for a prolonged recovery, or for whom more aggressive treatment or closer follow-up might be warranted. With more accurate outcome models, targeted treatment, and a better understanding of the factors that affect recovery, we may decrease morbidity in pediatric msTBI.

Our study has several limitations. While our sample size is similar to most published pediatric msTBI papers, it is not large, which limits interpretation of our results. Our sample size also precludes an in-depth examination of the effect of age on injury. Pubertal timing is another factor that would impact brain structure which we did not assess. Examining the impact of hormones and pubertal stage would be an important future contribution if large enough samples can be collected. Another limitation is the resolution of the MRS data. Mapping the MRS data to the dMRI data involved upsampling and some interpolation, which has the potential to give unreliable data. To compensate for this, we only examined averages within each tract, rather than element-wise data, which would have been less reliable. Additionally, the resolution was the same across all participants, so there was no bias that could influence group comparison. Our MRS sequence was also limited in the metabolites we could measure. Extracting other metabolites would aid interpretation. Unfortunately, there was a scanner change in the middle of the study, and while we have conducted comparison tests and controlled for scanner in our analyses, we cannot rule out that it may have impacted our results. Recent studies have shown some impact of time of scan, which was not controlled in this study. In future studies, we will use a new and improved MRS sequence that will allow us to measure additional metabolites reliably.

Here we show that differences in NAA correspond to differences in dMRI measures of WM organization, while choline did not show any correspondence. This suggests that demyelination plays an important role in WM disruption post-injury. Some of our results were unexpected, and raise questions that we intend to pursue in future studies, such as higher choline in the TBI-normal group. Higher choline in the group with the better outcome at the chronic time point could indicate recovery processes as it can be a marker of continual cellular turnover, but this question needs further research with additional variables. Lastly, we showed that the imaging variables assessed here jointly contribute to a more accurate outcome prediction than any variable individually. This highlights the importance of collecting multi-modal datasets. Future work including more patients and an improved EPSI sequence will further elucidate these effects.

CONFLICT OF INTEREST

Dr. Giza reports consultant fees from NFL-Neurological Care Program, NHLPA, serves on the advisory panel for the Major League Soccer, NBA, NCAA, US Soccer Federation, California State Athletic Commission, and has received speaker fees from Medical Education Speakers Network. Dr. Alger is the owner of NeuroSpectroScopics LLC.

ORCID

Emily L. Dennis http://orcid.org/0000-0001-7112-4009
Richard Mink http://orcid.org/0000-0002-7998-4713

REFERENCES

Akaike, H. (1974). A new look at the statistical model identification. *IEEE Transactions on Automatic Control*, 19(6), 716–723.

Ashwal, S., Babikian, T., Gardner-Nichols, J., Freier, M.-C., Tong, K. A., & Holshouser, B. A. (2006). Susceptibility-weighted imaging and proton magnetic resonance spectroscopy in assessment of outcome after pediatric traumatic brain injury. *Archives of Physical Medicine and Rehabilitation*, 87(12), 50–58.

Ashwal, S., Holshouser, B., Tong, K., Serna, T., Osterdock, R., Gross, M., & Kido, D. (2004). Proton spectroscopy detected myoinositol in children with traumatic brain injury. *Pediatric Research*, 56(4), 630–638.

Ashwal, S., Holshouser, B. A., Shu, S. K., Simmons, P. L., Perkin, R. M., Tomasi, L. G., ... Hinshaw, D. B. (2000). Predictive value of proton magnetic resonance spectroscopy in pediatric closed head injury. *Pediatric Neurology*, 23(2), 114–125.

Avants, B. B., Tustison, N. J., Song, G., Cook, P. A., Klein, A., & Gee, J. C. (2011). A reproducible evaluation of ANTs similarity metric performance in brain image registration. *NeuroImage*, 54(3), 2033–2044.

Babikian, T., Alger, J. R., Ellis, M. U., Giza, C., Dennis, E., Olsen, A., ... Asarnow, R. F. (2018). Whole brain magnetic resonance spectroscopic determinants of functional outcomes in pediatric moderate/severe traumatic brain injury. *Journal of Neurotrauma*, In Press.

Babikian, T., & Asarnow, R. (2009). Neurocognitive outcomes and recovery after pediatric TBI: Meta-analytic review of the literature. *Neuropsychology*, 23(3), 283–296.

Babikian, T., Freier, M. C., Ashwal, S., Riggs, M. L., Burley, T., & Holshouser, B. A. (2006). MR spectroscopy: Predicting long-term neuropsychological outcome following pediatric TBI. *Journal of Magnetic Resonance Imaging*, 24(4), 801–811.

Babikian, T., Marion, S. D., Copeland, S., Alger, J. R., O'Neill, J., Cazalis, F., ... Hilleary, S. M. (2010). Metabolic levels in the corpus callosum and their structural and behavioral correlates after moderate to severe pediatric TBI. *Journal of Neurotrauma*, 27(3), 473–481.

Benjamini, Y., Hochberg, Y. (1995). Controlling the false discovery rate: A practical and powerful approach to multiple testing. *Journal of the Royal Statistical Society Series B*, 57(1), 289–300.

Brenner, T., Freier, M. C., Holshouser, B. A., Burley, T., & Ashwal, S. (2003). Predicting neuropsychologic outcome after traumatic brain injury in children. *Pediatric Neurology*, 28(2), 104–114.

Catani, M., Allin, M. P., Husain, M., Pugliese, L., Mesulam, M. M., Murray, R. M., & Jones, D. K. (2007). Symmetries in human brain language pathways correlate with verbal recall. *Proceedings of the National Academy of Sciences*, 104(43), 17163–17168.

Cecil, K. M., Hills, E. C., Sandel, M. E., Smith, D. H., McIntosh, T. K., Mannon, L. J., ... Lenkinski, R. E. (1998). Proton magnetic resonance spectroscopy for detection of axonal injury in the splenium of the corpus callosum of brain-injured patients. *Journal of Neurosurgery*, 88(5), 795–801.

Delis, D. C., Kaplan, E., & Kramer, J. H. (2001). *Delis–Kaplan executive function system (D-KEFS)*. San Antonio, TX: Psychological Corporation.

Delis, D. C., Kramer, J. H., Kaplan, E., & Ober, A. (1994). *California Verbal Learning Test-Children's Version (CVLT-C)*. San Antonio, TX: Manual Psychological Corporation.

Dennis, E., Babikian, T., Giza, C., Thompson, P., & Asarnow, R. (2018). Neuroimaging of the injured pediatric brain: Methods and new lessons. *The Neuroscientist*, In Press.

Dennis, E. L., Babikian, T., Giza, C. C., Thompson, P. M., & Asarnow, R. F. (2017). Diffusion MRI in pediatric brain injury. *Child's Nervous System*, 33(10), 1683–1692.

Dennis, E. L., Ellis, M. U., Marion, S. D., Jin, Y., Moran, L., Olsen, A., ... Asarnow, R. F. (2015). Callosal function in pediatric traumatic brain injury linked to disrupted white matter integrity. *Journal of Neuroscience*, 35(28), 10202–10211.

Dennis, E. L., Jin, Y., Villalon-Reina, J., Zhan, L., Kernan, C., Babikian, T., ... Giza, C. C. (2015b). White matter disruption in moderate/severe pediatric traumatic brain injury: Advanced tract-based analyses. *NeuroImage Clinical*, 12(7), 493–505.

Dennis, E., Faskowitz, L., J., Rashid, F., Babikian, T., Mink, R., Babbitt, C., Johnson, J., ... Asarnow, R. F. (2017a). Diverging volumetric

trajectories following pediatric traumatic brain injury. *NeuroImage Clinical*, 15, 125–135.

Dennis, E., Rashid, L., F., Ellis, M. U., Babikian, T., Villalon-Reina, J. E., Jin, Y., Olsen, A., ... Asarnow, R. F. (2017b). Diverging white matter trajectories in children after traumatic brain injury: The RAPBI study. *Neurology*, 88(15), 1392–1399.

Ebel, A., & Maudsley, A. A. (2003). Improved spectral quality for 3D MR spectroscopic imaging using a high spatial resolution acquisition strategy. *Magnetic Resonance Imaging*, 21(2), 113–120.

Ellis, M. U., Marion, S. D., McArthur, D. L., Babikian, T., Giza, C., Kernan, C. L., ... Asarnow, R. F. (2015a). The UCLA study of children with moderate-to-severe traumatic brain injury: Event-related potential measure of interhemispheric transfer time. *Journal of Neurotrauma*, In Press.

Ellis, M. U., Marion, S. D., McArthur, D. L., Babikian, T., Giza, C., Kernan, C. L., ... Asarnow, R. F. (2015b). The UCLA study of children with moderate-to-severe traumatic brain injury: Event-related potential measure of interhemispheric transfer time. *Journal of Neurotrauma*, 33(11), 990–996.

Ghosh, N., Holshouser, B., Oyoyo, U., Barnes, S., Tong, K., ... Ashwal, S. (2017). Combined Diffusion Tensor and Magnetic Resonance Spectroscopic Imaging Methodology for Automated Regional Brain Analysis: Application in a Normal Pediatric Population. *Dev Neurosci*, 39, 413–429.

Holshouser, B. A., Ashwal, S., Luh, G. Y., Shu, S., Kahlon, S., Auld, K. L., ... Hinshaw, D. B. Jr. (1997). Proton MR spectroscopy after acute central nervous system injury: Outcome prediction in neonates, infants, and children. *Radiology*, 202(2), 487–496.

Holshouser, B. A., Tong, K. A., & Ashwal, S. (2005). Proton MR spectroscopic imaging depicts diffuse axonal injury in children with traumatic brain injury. *AJNR. American Journal of Neuroradiology*, 26, 1276–1285.

Jin, Y., Shi, Y., Jahanshad, N., Aganj, I., Sapiro, G., Toga, A. W., & Thompson, P. M. (2011). *3D elastic registration improves HARDI-derived fiber alignment and automated tract clustering. 8th Proc IEEE Int Symp Biomed Imaging*. Chicago, IL: IEEE. p 822–826.

Jin, Y., Shi, Y., Zhan, L., Gutman, B. A., de Zubicaray, G. I., McMahon, K. L., ... Thompson, P. M. (2014). Automatic clustering of white matter fibers in brain diffusion MRI with an application to genetics. *NeuroImage*, 100, 75–90.

Keenan, H. T., & Bratton, S. L. (2006). Epidemiology and outcomes of pediatric traumatic brain injury. *Developmental Neuroscience*, 28(4–5), 256–263.

Li, B. S., Wang, H., & Gonen, O. (2003). Metabolite ratios to assumed stable creatine level may confound the quantification of proton brain MR spectroscopy. *Magnetic Resonance Imaging*, 21(8), 923–928.

Maudsley, A. A., Darkazanli, A., Alger, J. R., Hall, L. O., Schuff, N., Studholme, C., ... Zhu, X. (2006). Comprehensive processing, display and analysis for in vivo MR spectroscopic imaging. *NMR in Biomedicine*, 19(4), 492–503.

Maudsley, A. A., Govind, V., Levin, B., Saigal, G., Harris, L., & Sheriff, S. (2015). Distributions of magnetic resonance diffusion and spectroscopy measures with traumatic brain injury. *Journal of Neurotrauma*, 32(14), 1056–1063.

Moffett, J. R., Arun, P., Ariyannur, P. S., & Namboodiri, A. M. (2013). N-Acetylaspartate reductions in brain injury: Impact on post-injury neuroenergetics, lipid synthesis, and protein acetylation. *Frontiers in Neuroenergetics*, 5, 11.

Moran, L. M., Babikian, T., Del Piero, L., Ellis, M. U., Kernan, C. L., Newman, N., ... Asarnow, R. (2016). The UCLA study of predictors of cognitive functioning following moderate/severe pediatric traumatic brain injury. *Journal of the International Neuropsychological Society*, 22(05), 512–519.

Parry, L., Shores, A., Rae, C., Kemp, A., Waugh, M. C., Chaseling, R., & Joy, P. (2004). An investigation of neuronal integrity in severe paediatric traumatic brain injury. *Child Neuropsychology: A Journal on Normal and Abnormal Development in Childhood and Adolescence*, 10(4), 248–261.

Sabati, M., Sheriff, S., Gu, M., Wei, J., Zhu, H., Barker, P. B., ... Maudsley, A. A. (2015). Multivendor implementation and comparison of volumetric whole-brain echo-planar MR spectroscopic imaging. *Magnetic Resonance in Medicine*, 74(5), 1209–1220.

Shutter, L., Tong, K. A., & Holshouser, B. A. (2004). Proton MRS in acute traumatic brain injury: Role for glutamate/glutamine and choline for outcome prediction. *Journal of Neurotrauma*, 21(12), 1693–1705.

Sidaros, A., Engberg, A. W., Sidaros, K., Liptrot, M. G., Herning, M., Petersen, P., ... Rostrup, E. (2008). Diffusion tensor imaging during recovery from severe traumatic brain injury and relation to clinical outcome: A longitudinal study. *Brain: A Journal of Neurology*, 131(2), 559–572.

Song, S. K., Yoshino, J., Le, T. Q., Lin, S. J., Sun, S. W., Cross, A. H., & Armstrong, R. C. (2005). Demyelination increases radial diffusivity in corpus callosum of mouse brain. *NeuroImage*, 26(1), 132–140.

Walz, N. C., Cecil, K. M., Wade, S. L., & Michaud, L. J. (2008). Late proton magnetic resonance spectroscopy following traumatic brain injury during early childhood: Relationship with neurobehavioral outcomes. *Journal of Neurotrauma*, 25(2), 94–103.

Wechsler, D. (2003). *Wechsler intelligence scale for children–Fourth Edition (WISC-IV)*. San Antonio, TX: The Psychological Corporation.

Wilde, E. A., Ayoub, K. W., Bigler, E. D., Chu, Z. D., Hunter, J. V., Wu, T. C., ... Levin, H. S. (2012). Diffusion tensor imaging in moderate-to-severe pediatric traumatic brain injury: Changes within an 18 month post-injury interval. *Brain Imaging and Behavior*, 6(3), 404–416.

Yeo, R. A., Phillips, J. P., Jung, R. E., Brown, A. J., Campbell, R. C., & Brooks, W. M. (2006). Magnetic resonance spectroscopy detects brain injury and predicts cognitive functioning in children with brain injuries. *Journal of Neurotrauma*, 23(10), 1427–1435.

Zhang, Y., Zhang, J., Oishi, K., Faria, A. V., Jiang, H., Li, X., ... Mori, S. (2010). Atlas-guided tract reconstruction for automated and comprehensive examination of the white matter anatomy. *NeuroImage*, 52(4), 1289–1301.